



ELSEVIER

Geomorphology 44 (2002) 155–170

GEOMORPHOLOGY

www.elsevier.com/locate/geomorph

# Yardangs in the semiarid central sector of the Ebro Depression (NE Spain)

M. Gutiérrez-Elorza\*, G. Desir, F. Gutiérrez-Santolalla

*Dpto. Ciencias de la Tierra-Geomorfología, Facultad de Ciencias, Universidad de Zaragoza, 50009 Saragossa, Spain*

Received 7 June 2001; received in revised form 25 September 2001; accepted 26 September 2001

## Abstract

This work reveals the existence of yardangs in the central sector of the semiarid Ebro Depression of Spain. Almost all the documented yardang fields are located in extreme arid environments. The yardangs are developed in horizontal tertiary gypsum and limestone. More than 100 closed depressions (solution dolines) have been formed in the soluble sediments of this area, some of them hosting saline lakes or playas. All the yardangs occur on the leeward margin of the larger playas and their mean orientation (N122E) coincides with the prevalent direction of the strong local wind called *Cierzo*. Two main types of yardang have been identified; 44 rock yardangs formed in the Miocene bedrock and six yardangs developed in unconsolidated lacustrine deposits. Nebkha dunes have been recognized and yardang-like morphologies in building rubble accumulations on the floor of a playa (<100 years old). The generation of yardangs in this semiarid area is related to the presence of playas, which constitute the source of abrading particles during dry periods. At the present time, the yardangs developed in the lacustrine terraces, nebkhas and rubble accumulations are active landforms, whereas the rock yardangs are considered to be inactive. © 2002 Elsevier Science B.V. All rights reserved.

*Keywords:* Yardang; Playa; Semiarid region; Ebro depression; Spain

## 1. Introduction

Yardangs are erosional landforms produced by wind action, and according to McCauley et al. (1977) are probably one of the least understood landforms of the Earth's surface. In the geomorphological literature, yardang is generally used to designate elongate streamlined hills developed in different lithologies in numerous deserts of the world (Halimov and Fezer,

1989; Goudie, 1999; Goudie et al., 1999). The term yardang corresponds to a local word introduced by Hedin (1903) in his study of the Taklimakan Desert in the east of China. The initial investigations of yardangs had a local character and were focused mainly on their description rather than on their genesis. The use of airborne imagery such as aerial photographs (Maingnet, 1968, 1972) and satellite images for the study of yardang fields both on planet Earth and on Mars gave rise to a significant advance in the authors' knowledge (McCauley, 1973; Ward, 1979). These analyses have been complemented by laboratory experiments, field observations, and theoretical considerations (Whitney, 1978, 1983; Ward and Greeley, 1984).

\* Corresponding author. Tel.: +34-76-761092; fax: +34-76-761088.

*E-mail address:* mgelorza@posta.unizar.es (M. Gutiérrez-Elorza).

From the interpretation of satellite images, McCauley et al. (1977) identified the largest yardang fields on Earth. All of them are located in hyperarid areas and some of them cover as much as 650,000 km<sup>2</sup> (Mainguet, 1968), as in the area southeast and southwest of the Tibesti Massif (Borkou, central Sahara). The numerous investigations of the origin of the yardangs reveal that their generation resulted from the combined effects of several processes: wind abrasion, deflation, gullying and slope movements. Several excellent review works go deeply into different aspects of these peculiar morphologies (Whitney, 1985; Cooke et al., 1993; Laity, 1994; Breed et al., 1997).

The principal aim of this work is to reveal the existence of a suite of yardangs associated with playas in the central sector of the Ebro Depression (Spain). These are the northernmost yardangs reported in (around 45°N in latitude). These yardangs are found in an area with semiarid climate, whereas all the other documented yardang fields are located in extremely arid environments with almost no vegetation cover, except Rogers Lake (USA) with a mean annual rain-

fall of 149 mm (Lancaster, personal communication). On the other hand, this work analyses the processes (past and present) which have given rise to these landforms and establishes the geomorphological evolution of playa–yardang systems.

## 2. The study area

The study area is located in the central sector of the Ebro Depression, NE Spain (Fig. 1). It is situated 50 km to the southeast of Zaragoza City and 5 km to the south of Bujaraloz village, forming part of a semiarid region called Los Monegros. The sedimentary fill in this sector of the Ebro Tertiary Basin is made up of horizontally lying Oligo-Miocene continental sediments. The playa–yardang systems are developed on an exhumed structural platform (around 320–350 m a.s.l.). This platform is located between the Miocene sediments of Santa Quiteria Sierra (574 m) to the north, and the deeply entrenched meandering Ebro River, which flows 200 m below the platform 4–15 km to the south, in the Sástago area (Fig. 2). The

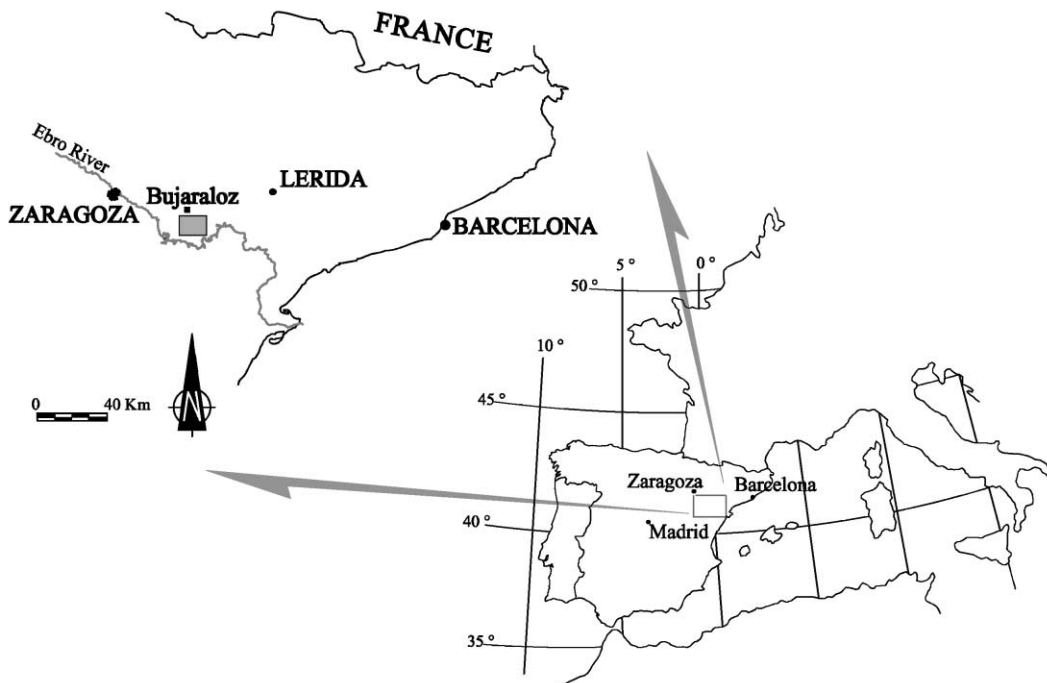


Fig. 1. Location of the study area.

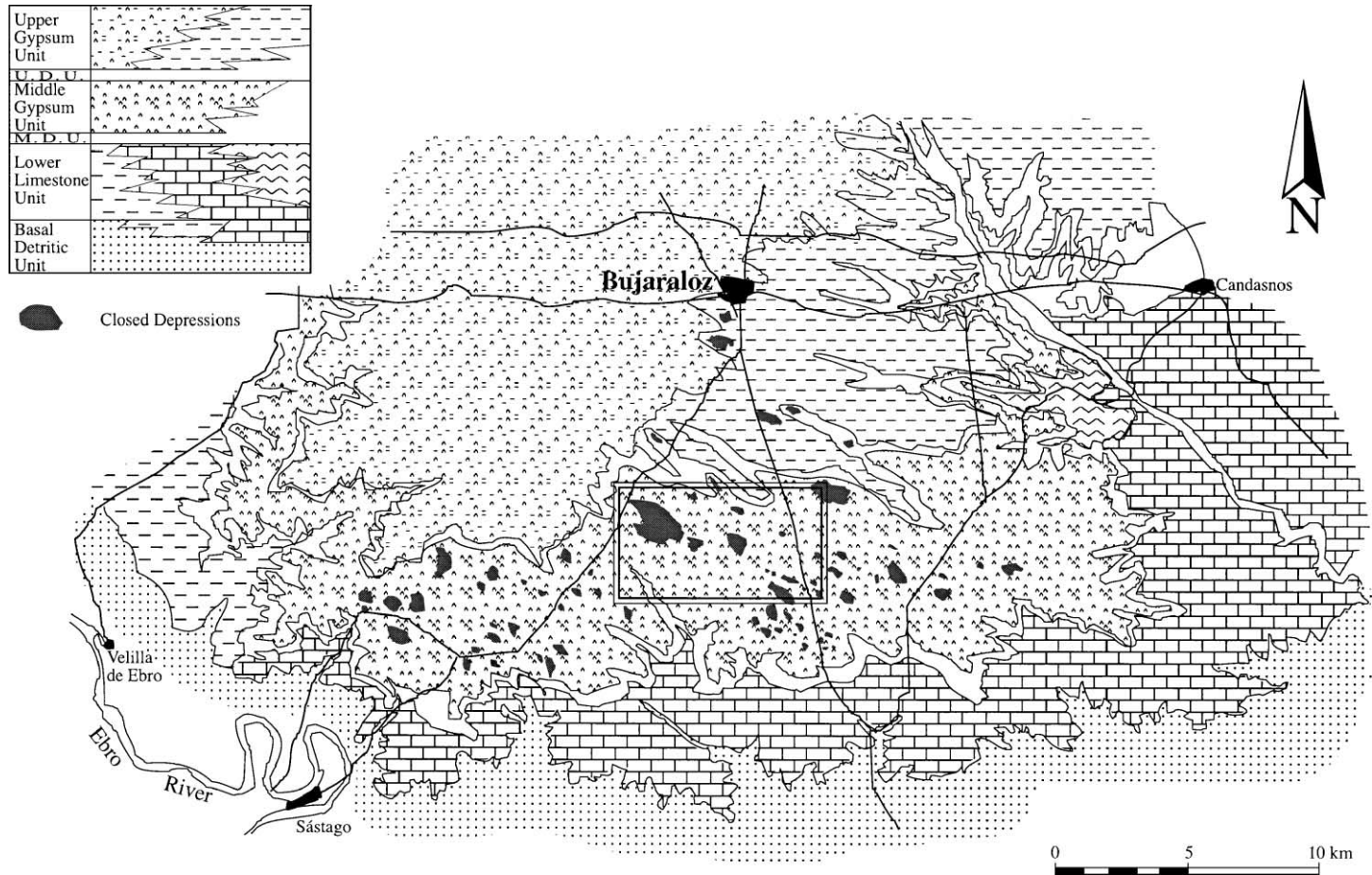


Fig. 2. Geological setting of the study area modified (Salvany et al., 1996). U.D.U.: Upper Detritic Unit. M.D.U.: Middle Detritic Unit.

subhorizontal topography of the platform is interrupted by over 100 closed depressions. These closed basins show extremely flat bottoms and may have scarped or gentle margins. Most of the depressions are strongly elongated and preferentially orientated in the WNW–ESE direction. The flat bottoms of some of the deepest basins host saline lakes or playas, called *saladas* in the region, with precipitation of evaporite minerals (Fig. 3).

The exhumed Bujaraloz platform is underlain by Lower Miocene gypsum and limestone sediments (Fig. 2) described by Salvany et al. (1994a,b, 1996). These sediments, form part of the Bujaraloz–Sariñena Unit (Ramírez, 1997; Solá and Costa, 1997) and the gypsum lithofacies, correspond to the Yesos de Retuerta Unit of the Zaragoza Gypsum Formation (Quirantes, 1978). The larger closed depressions (up to 2.49 km<sup>2</sup> in area) occur in the western sector of the platform where the gypsum sediments are thicker (around 40 m). Towards the east, the gypsum lithofacies interfingering with limestone are thinner and the number and size of the depressions decreases.

The mean annual temperature and precipitation in Bujaraloz meteorological station are 14.5 °C and 400 mm, respectively. Potential evapotranspiration of 778 mm has been estimated for the area (Liso and Ascaso, 1969) indicating semiarid conditions. The wind and

aeolian energy have been studied in detail during 3 years at an anemometric station installed in the proximity of Bujaraloz village (Puircerús et al., 1994). The record shows that the strong wind, locally known as *Cierzo*, preferentially blows during the spring and winter with a dominant WNW to ESE directions (Fig. 4A). This wind develops most of the kinetic energy,  $E = 1/2\rho v^2$  ( $\rho$  is the air density) (Fig. 4B). Mean speeds of 4.5, 5.5 and 6 m/s at 10, 30 and 50 m in height, respectively, have been recorded in the anemometric station. The maximum speed measured in the Zaragoza Meteorological station reached 38 m/s (136 km/h) with WNW winds, in 1979. The *Cierzo* is a dry and gusty wind which is channelled in the direction of the Ebro River valley when there is an atmospheric pressure gradient between the Cantabrian (Atlantic) and Mediterranean seas (Ascaso and Cuadrat, 1981).

The origin of the closed depressions in the Bujaraloz platform has been explained by an evolutionary model established by Sánchez et al. (1998). According to this model, the closed depressions initially formed by the structurally controlled dissolution of the bedrock by infiltrating waters (solution dolines). The infiltration of the rainfall is favoured by the horizontal topography of the platform (Ibáñez, 1975), whereas the karstification of the bedrock is controlled by a



Fig. 3. General view of the ephemeral saline lake of La Playa. Foreground, abandoned salts exploitation.

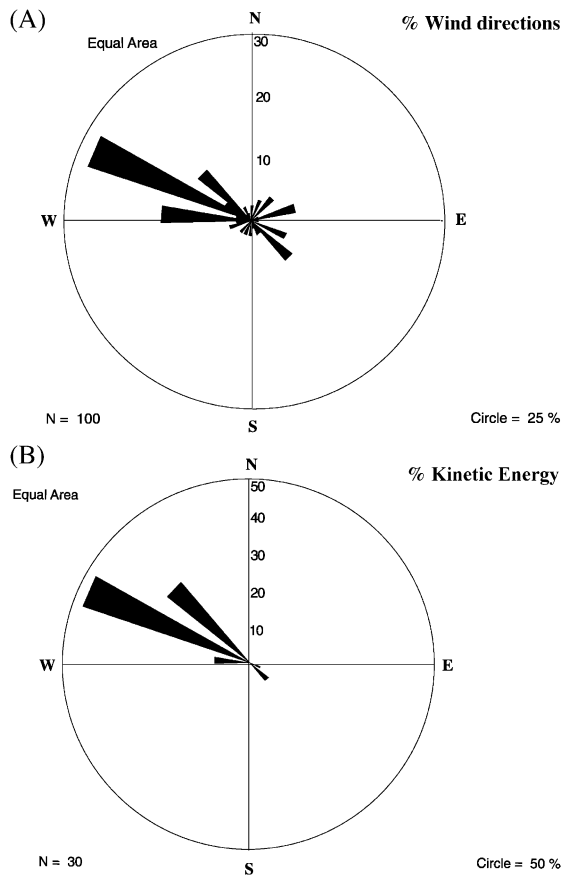


Fig. 4. (A) Frequency distribution of wind directions (%). (B) Kinetic energy (%).

fracture set (Quirantes, 1965, 1978; Arlegui and Soriano, 1996, 1998; Arlegui and Simón, 2001).

Most of the water and solute input to the playas is supplied by groundwater flows which tend to concentrate along joints and solutionally enlarged discontinuities (Sánchez Navarro et al., 1989; Sánchez et al., 1998; García Vera, 1996). According to Pueyo (1978–1979), the brines of the playas are of the Cl–SO<sub>4</sub>–Na–(Mg) type (Eugster and Hardie, 1978). In winter, the precipitation of mirabilite (Na<sub>2</sub>SO<sub>4</sub>·10H<sub>2</sub>O) predominates. In spring and autumn, algal mats, 3–4 mm thick, form in the bed of the flooded areas. Beneath this bed, there is a black sapropelic layer rich in decomposing organic matter (Pueyo, 1980). The salts form by desiccation during spring and summer. During dry periods, the salt is evacuated by the prevailing WNW–ESE winds (Ibáñez, 1975; Pueyo, 1978–

1979; Sánchez Navarro et al., 1989). The evaporation enhanced by the dry winds gives rise to cracks and polygons on the lake floor.

The playas have a characteristic fauna represented by crustaceans, including *Artemia* sp., copepods and ostracods, as well as protozoans and flagellated algae. The periphery is colonised by halophilous vegetation (*Salicornia* sp.) and frequently shows saline efflorescences formed by capillary rise (Pueyo, 1980). On the other hand, some of the playas have an external periphery modified by agricultural practices.

### 3. Results

To study the playa–yardang systems, a preliminary geomorphological map of the study area was pro-

duced by interpretation of aerial photographs of 1:18,000 and 1:33,000 scales. All the recognisable yardang-like morphologies were represented in this map. Subsequently, a detailed field survey of the area was carried out. All the mapped yardang morphologies were carefully checked and analysed in situ in order to gain information about their geometry, morphometry, and spatial relationship with other geomorphological and sedimentary features. Additionally, a detailed geomorphological map of the largest closed depressions was made in the field on a 1:5000 scale topographic map with contour intervals of 1 m. This map includes a precise representation of the lacustrine terraces and the aeolian morphologies identified in the field. Combining the maps produced in the field and by stereoscopic analysis of the airborne imagery, a final geomorphological map was delineated on the 1:5000 topography. A synthetic sketch derived from this map is shown in Fig. 5. The grain size and carbonate content of several samples collected from terraces, yardang slopes, corridors, and playa bottoms were analysed in the laboratory.

The spatial association between the yardangs and the closed depressions indicates a genetic interrelation between both landforms. All the yardangs are located at the leeward strip of the ephemeral saline lakes, especially linked to the larger ones: La Playa, El Pueyo and El Pito (Fig. 5). The yardangs are developed primarily in Miocene gypsum beds, although limestone is exposed in some of them. In the slopes of the yardangs, the nodules of alabastrine gypsum show well-developed solution features (*rillenkarren* and *napfkarren*). In the gypsum blocks on the playa surface, these karrens are developed only in the leeward sides, whereas the abrading action of the wind dominates in the windward side. The surface of the yardangs is colonised by sparse shrub vegetation, dominantly composed by *Rosmarinus officinalis*, *Genista scorpius* and *Thymus vulgaris*.

Up to 50 yardangs have been identified in the study area. They can be grouped in two types (Table 1). Forty-four yardangs are developed in Miocene bedrock (rock yardangs) and six have been recognized in the unconsolidated lacustrine deposits. The mean direction of the yardangs, N122E (Fig. 6A), coincides with the most frequent wind direction (Fig. 4A). There is no consistent relationship between the orientation of the yardangs and the strike of the joints measured in

four locations within the study area (Fig. 6B). However, several authors reveal the significant role played by the WNW–ESE fractures in the morphogenesis of the central sector of the Ebro Depression (Quirantes, 1965; Gutiérrez et al., 1994; Arlegui and Soriano, 1998; Maldonado et al., 2000). According to Arlegui and Simón (2001), the generation of the WNW–ESE joint sets is related to perturbations in the stress field induced by pre-existing N–S trending joints.

The maximum length, width and height of the yardangs are 264, 40 and 17 m, respectively (Table 1). The average length/width ratio is 4.1:1 (Fig. 7). These proportions are in agreement with the values obtained in yardang forms generated by experimental studies in wind tunnels (Ward and Greeley, 1984) and differ from the 10:1 ratios calculated by Mainguet (1968, 1972) for the yardangs of the Borkou area in the Sahara Desert. The elongated and aerodynamic shape of these aeolian landforms minimises the resistance to the wind flow. The studied yardangs correspond to the meso- and mega-yardangs of Cooke et al. (1993) and to yardangs and mega-yardangs following the terminology of Livingstone and Warren (1996).

In the northeastern sector of the bottom of La Playa saline lake, several yardang-like morphologies have been developed on rubbish dump material, constituted mainly by gypsum blocks. These currently active morphologies show an approximate E–W orientation. The erosion of the rubble has given rise to streamlined deposits consisting of gypsum clasts with a matrix of gypsiferous silts.

The windward and leeward slopes of the yardangs have mean angles of 30° and 6°, respectively (Fig. 8). The slopes generally show a stepped profile controlled by the horizontal bedding of the bedrock, similar to the yardangs described in the coastal desert of central Perú (McCauley et al., 1977). The windward slope is always steep, whereas the incline of the leeward slope shows a progressive decline towards the downwind extreme. Signs of undercutting at the foot of the slopes are very scarce, indicating that, at the present time, sediment accumulation exceeds wind deflation and abrasion (sandblasting). However, the gypsiferous silts slope deposits locally show aeolian pits and flutes. The pits are small (2–5 cm) irregular, closed depressions, which commonly occur on steep slopes. The flutes have a U-like shape in plain view and open in the downwind direction (McCauley et al., 1979;

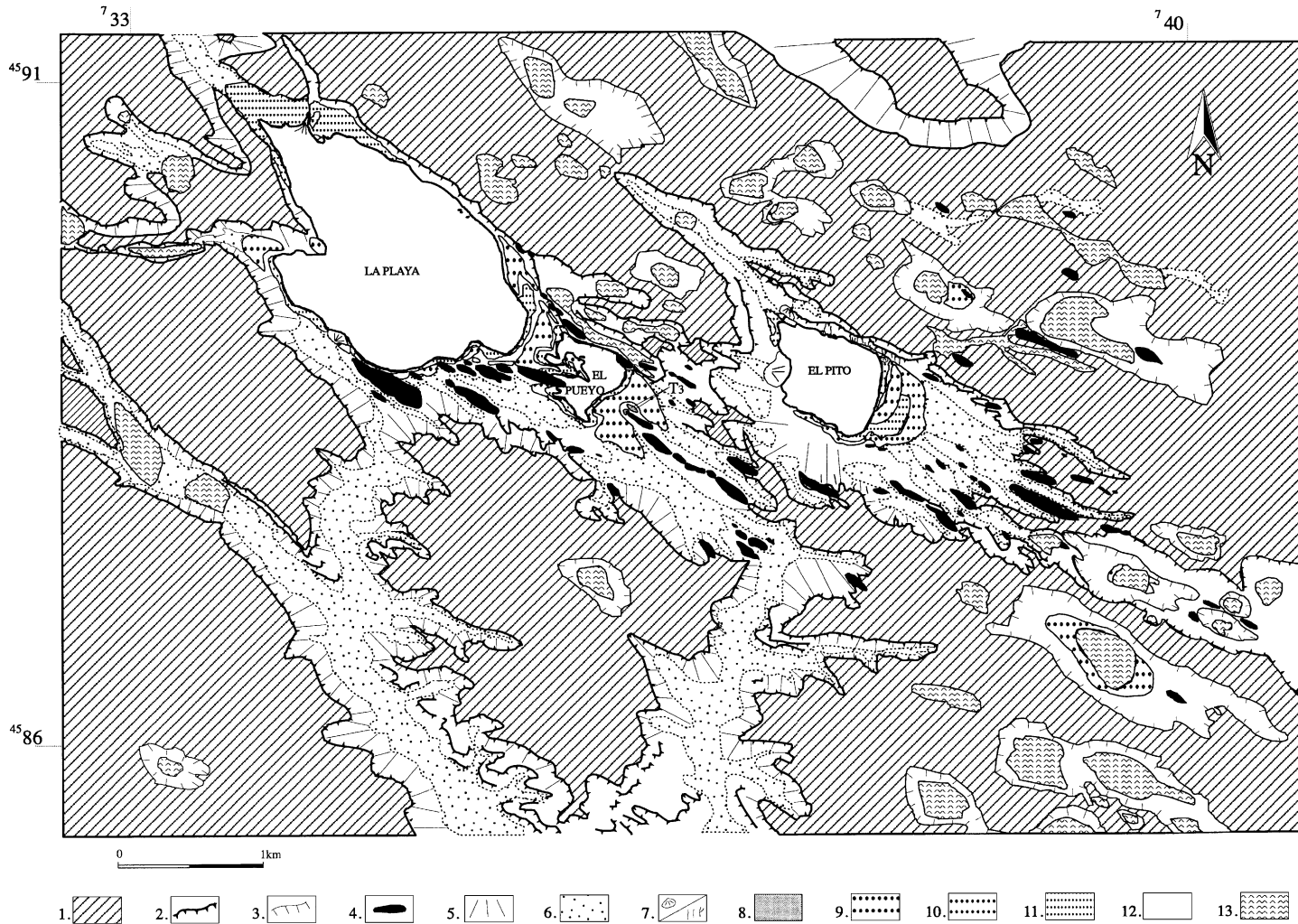


Fig. 5. Geomorphological map of the playa–yardang systems located about 5 km to the south of Bujaraloz village: (1) structural platform; (2) scarps; (3) edge of closed depressions; (4) single yardangs; (5) slope deposits; (6) corridors and flat bottom infilled valleys; (7) alluvial fans and gullies; (8) lacustrine terrace  $T_3$ ; (9) lacustrine terrace  $T_{2a}$ ; (10) lacustrine terrace  $T_{2b}$ ; (11) lacustrine terrace  $T_1$ ; (12) playa bottom; (13) bowl-shaped dolines.

Table 1  
Morphometric analysis and main yardang types

Number	Direction	Length	Width	Height	Ratio l/w	Slope		Corridor		Type				
						Windward	Leeward	Maximum Width	Slope	Mesa	Saw tooth crest	Cone	Keel	Ridge to platform
1	123	136	40	13	3.4	26.5	3.3	44	3.0	x				
2	125	34	8	3	4.3	14.0	4.0	30	2.6					x
3	115	40	12	7.5	3.3	30.3	8.1	70	5.7			x		
4	111	48	20	9.5	2.4	33.7	14.0	70	5.7		x			
5	116	120	20	6	6.0	20.6	0.3	56	2.3					x
6	110	76	26	9	2.9	35.0	5.7	56	2.3	x				
7	113	42	16	7	2.6	56.3	14.0	120	1.8				x	
8	112	140	26	10.5	5.4	29.1	19.7	120	1.8		x			
9	128	30	14	3	2.1	39.8	9.5	–	–	x				
10	119	54	12	2.5	4.5	63.4	9.1	–	–		x			
11	116	44	14	4.2	3.1	21.8	26.6	10	5.7				x	
12	130	22	3	1.2	7.3	29.9	1.9	–	–		x			
13	111	16	10	2	1.6	45.0	14.0	30	0.0	x				
14	124	26	10	3	2.6	14.0	6.7	16	4.8			x		
15	125	18	10	2.5	1.8	29.1	3.7	16	4.8				x	
16	122	20	8	1.5	2.5	37.8	7.6	–	–	x				
17	123	70	10	2.5	7.0	26.5	2.6	12	18.0		x			
18	136	56	20	10	2.8	41.8	3.6	150	1.4					x
19	125	94	22	9	4.3	16.6	1.6	150	1.4				x	
20	120	240	26	13	9.2	25.7	5.7	72	2.1					x
21	121	92	20	6	4.6	31.0	10.6	80	2.1		x			
22	128	74	18	6	4.1	39.8	7.1	8	6.3	x				
23	126	34	12	3	2.8	36.9	5.7	14	4.1	x				
24	106	20	8	0.5	2.5	14.0	2.9	–	–				x	
25	111	50	16	1	3.1	39.8	1.1	–	–	x				
26	130	264	30	11	8.8	32.0	2.9	36	3.2					x
27	142	48	8	3	6.0	14.0	1.7	30	5.0					x
28	138	36	10	3.5	3.6	20.6	2.6	30	5.0				x	
29	134	90	20	11	4.5	20.6	1.1	44	4.8					x
30	133	24	8	2	3.0	26.6	2.7	20	4.3					x
31	131	24	10	2	2.4	18.4	1.8	36	8.4				x	
32	145	64	16	11	4.0	20.6	3.3	20	8.5					x
33	110	44	14	3.2	3.1	14.0	9.5	24	7.8		x			
34	116	84	16	9	5.3	30.3	1.0	30	3.2					x
35	123	206	34	15	6.1	18.4	0.9	30	3.7					x
36	115	174	30	4	5.8	26.6	10.2	–	–		x			
37	122	68	24	2.6	2.8	14.0	2.6	–	–				x	
38	138	52	18	11.4	2.9	38.7	3.2	–	–					x
39	118	62	24	8	2.6	39.9	6.6	–	–				x	
40	120	32	14	1.4	2.3	43.9	2.9	–	–				x	
41	123	84	24	8.9	3.5	17.7	2.3	40	2.4					x
42	125	132	28	17	4.7	56.3	1.0	–	–					x
43	112	36	14	11	2.6	51.3	14.0	36	3.3				x	
44	122	46	12	7	3.8	26.6	2.0	–	–					x
1 <sup>a</sup>	155	16	10	2.5	1.6	25.6	11.9	–	–				x	
2 <sup>a</sup>	99	14	6	1.8	2.3	36.9	26.6	–	–				x	
3 <sup>a</sup>	153	20	12	1	1.7	26.6	9.5	–	–	x				
4 <sup>a</sup>	105	36	8	2.3	4.5	14.0	7.1	–	–	x				
5 <sup>a</sup>	142	50	8	3.5	6.3	36.9	14.0	–	–	x				
6 <sup>a</sup>	103	30	14	3.9	2.1	45.0	20.6	–	–	x				
Mean	122.6	72.0	17.2	6.3	4.0	30.2	5.9	48.4	4.4					

<sup>a</sup> Lacustrine deposits.



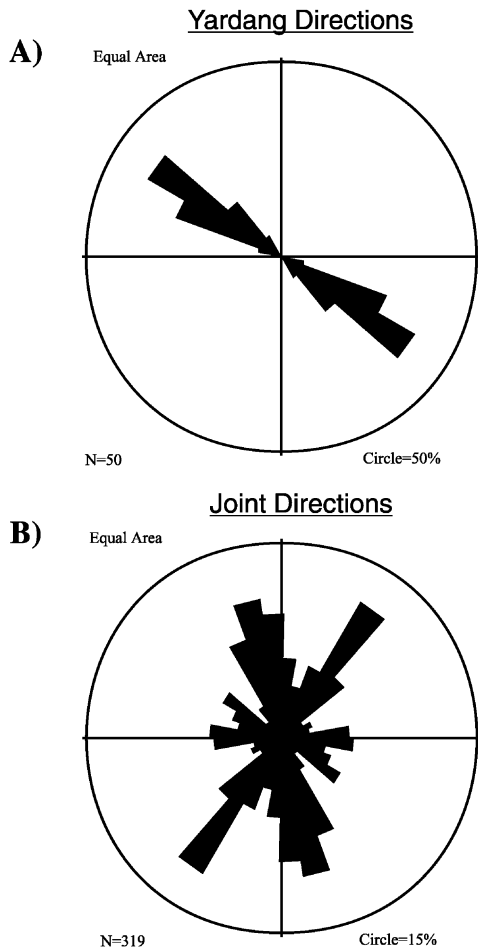


Fig. 6. (A) Frequency of yardang directions. (B) Frequency of joint directions measured in four stations of the study area.

Whitney, 1983; Laity, 1995). These deposits also show flakes of a thin surficial crust detached by the wind, exposing cohesionless sediments to the erosive action of the wind. These features are observed only on broad surfaces devoid of vegetation.

The sandy limestone outcropping in the windward slopes of the yardangs shows alveoles and occasionally, some tafoni. There are also flakes and salt efflorescences produced by capillary rise. Planar and angular clasts, whose major axis (2 cm) is preferentially oriented parallel to the wind direction, are found in La Playa and El Pueyo. Some of these clasts may be suspended above the surface forming micro-pedestal or micro-hoodoo like micromorphologies. On

the other hand, on the leeward side of the yardangs, there commonly is an accumulation of lenticular gypsum crystals.

The flanks of the yardangs show convex–concave slopes that are actually covered by vegetation (Fig. 8). At the present time, the main process on the slopes is sheet flow conditioned by the obstacles constituted by the vegetation. The differential weathering between the gypsum and limestone beds generates undercuts that finally give rise to small limestone rock-falls. Very likely, dissolution processes and salt weathering contribute to the erosion of the bedrock. The lower part of the slopes is generally covered by gypsiferous silts (weathering products of the Miocene gypsum) with limestone blocks and regosols. The thickness of these deposits increases towards the corridors and flat-bottom infilled valleys developed between the yardangs.

In the elongated depression between La Playa and El Pueyo, the slopes of the yardangs located on north and south margins show a high inclination converging towards the axis of the depression. The corridors, with a WNW–ESE orientation (Fig. 5), have a mean width of 48 m and a mean slope towards the closed depressions close to 4° (Table 1). The infill of the corridors is composed of gypsiferous silts with scattered angular limestone clasts. Some corridors have diffuse-edged closed depressions. Very likely, they have been generated by subsidence caused by the dissolution of the evaporite bedrock, although aeolian deflation may also contribute to their formation.

Most of the rock yardangs show flat tops controlled by the horizontal structure of the bedrock. The yardangs have been grouped following the morphological classification established by Halimov and Fezer (1989)

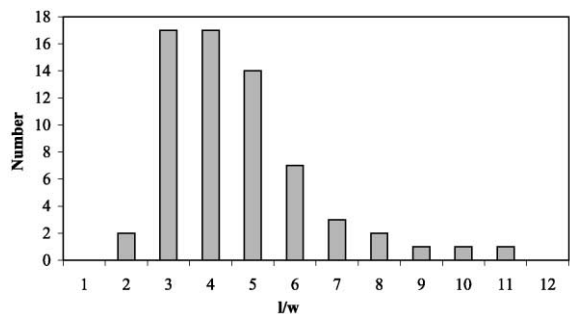


Fig. 7. Frequency distribution of width/length ratio of all yardangs.



Fig. 8. Keel-yardang developed in the Miocene gypsiferous deposits. In the background, La Playa lake basin, the exhumed Bujaraloz platform and the overlying Miocene sediments in Santa Quiteria Sierra. Arrow indicates wind direction.

from their studies in central Asia. Several morphological types have been identified in the study area: ridge-yardangs associated with platforms which constitute elongated appendixes of the platforms (linked on the

leeward side to the platform surfaces); mesa-yardangs controlled by runoff incision; cone-yardangs resulting from the parallel retreat of the slopes of the mesas; saw-tooth crest-yardangs generated by the differential ero-



Fig. 9. Yardang developed in the deposits of the lacustrine terrace  $T_2$  of the La Playa-El Pueyo ephemeral lakes. Arrow indicates wind direction.

sion of the bedrock in the crest and keel-yardangs which have the shape of an upturned ship. According to Table 1, the dominant morphologic type is the ridge-yardang associated with platforms. The Halimov and Fezer (1989) classification also introduces a cyclic concept in the development of these landforms. It is difficult to share this cyclic idea since it does not consider the structural factor (mesas and hogbacks) in the evolution of the yardangs.

The yardangs developed on lacustrine terrace deposits are located in the western margin of El Pueyo playa. These keel-type yardangs have been formed in the two older terraces (Fig. 9).

There are three playas in the surveyed area (Fig. 5) called La Playa (Fig. 2), El Pueyo and El Pito, whose bottoms cover 1.72, 0.14 and 0.35 km<sup>2</sup> in area, respectively. They have scarped northwestern margins, which may be incised by gullies covered by vegetation suggesting limited water runoff and sediment supply

to the lakes. Locally, there are small debris cones at the boundary between the corridors and the lake. The southeastern margins generally show more gentle slopes.

These lakes are commonly flooded during the cold periods of the year since evaporation then diminishes considerably. The only limnometric data available have been recorded in La Playa during the period 1993–1997. The depth ranged from 51 to 25 cm and 35 cm was the average depth. The rest of the lakes have shallower depths (Castañeda, personal communication). Commonly, by the end of spring and at the beginning of summer, the lakes are totally dry and covered with an evaporite crust. During these dry periods, the particles from the playa bed can be deflated, conferring an abrasive character to the wind. Other particles can come from a distance, away from the playas.

The aerial photographs show how the southeastern sector of the bed of the playas is higher than the rest of

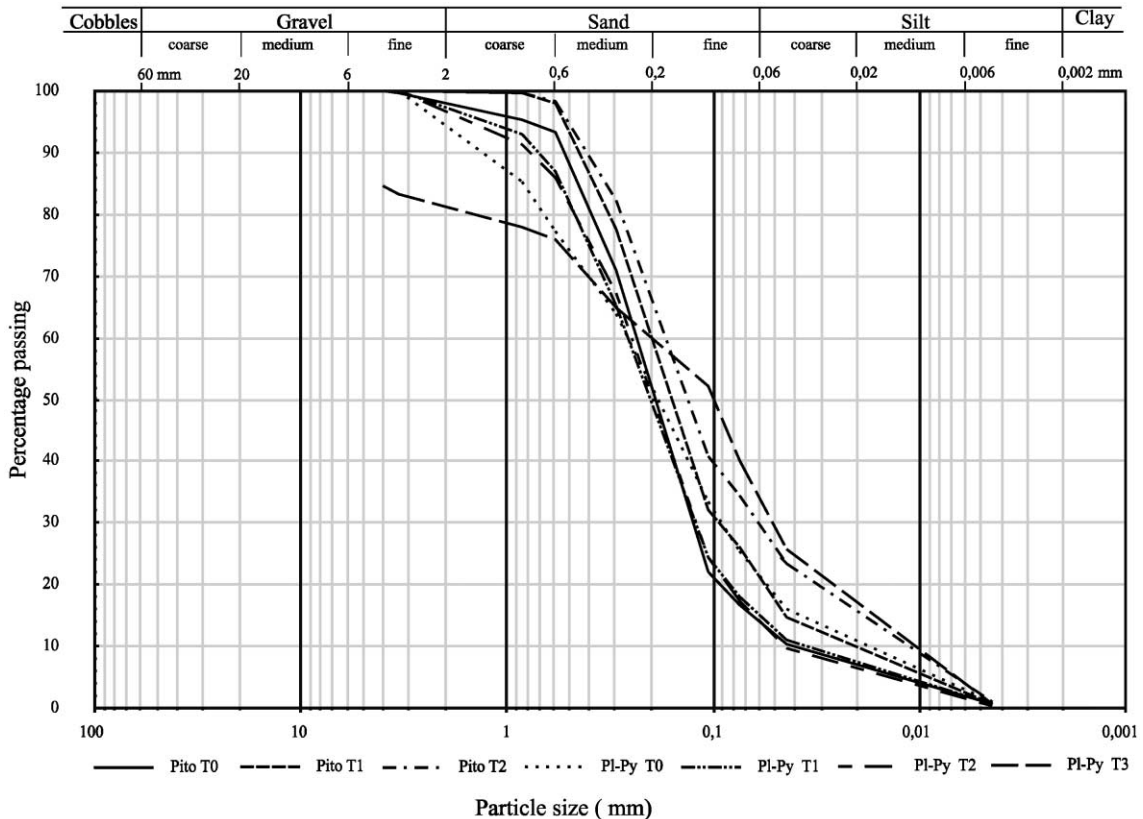


Fig. 10. Grain-size curves of the deposits of the lake terraces and bottoms.

the lake bottoms. Probably, in the downwind sector of the lakes there is a higher aggradation rate by wave action and by aeolian supply. These accumulations show different geometries in the 1956 and 1980 aerial photographs.

Three stepped levels of lacustrine terraces have been differentiated (Fig. 5). They show a broad development in the southeastern sector of the larger playas (La Playa, El Pueyo and El Pito). The oldest level ( $T_3$ ), at 7.5 m above the current playa bed and 4 m thick, is represented by two small surfaces to the southeast of El Pueyo playa. The intermediate terrace ( $T_2$ ), at 3.5–3 m above the playa bed, is the surface with greatest extent. It reaches more than 3 m in thickness. In El Pito playa, this terrace ( $T_2$ ) shows two levels ( $T_{2a}$  and  $T_{2b}$ ) incised 20 cm one in the other. These levels are also recognised NW of La Playa. The base of these deposits is not exposed since it is overlapped by either the sediments of the youngest terrace or by the deposits of the lake bottom. In El Pueyo Lake, the  $T_2$  terrace has been locally remoulded into yardangs (Fig. 9). The most recent terrace ( $T_1$ ) is located at 0.3–0.5 m above the playa. Its deposit, more than 0.4 m thick, is overlapped by the sediments of the current lake bottom.

The yardang slopes are locally overlapped by the deposits of the two highest terraces. In La Playa lake basin, some corridors are connected with the  $T_2$  surface. The terrace sediments are made up of white-grey coloured, fine-grained deposits showing a crude horizontal stratification. The grain-size analysis of the terrace deposits shows that fine sand is the dominant textural fraction (Fig. 10). They are composed of 87% lenticular gypsum crystals and 13% carbonate with some calcareous concretions. The  $T_2$  and  $T_1$  terraces are formed dominantly of fine sand and silt, whereas the  $T_3$  terrace is mainly formed by silt with a proportion of relatively coarse-grained particles.

In the outer fringe of the lake bottoms, there is an aureole of *Salicornia* sp. which traps wind blown particles. Commonly, on the windward side of these plants, there is a preferential accumulation of elongated limestone and gypsum clasts with the major axis oriented perpendicular to the wind direction. On the leeward side of the *salicornias*, the deposit is formed mainly of small lenticular gypsum crystals. In this fringe, there are also *nebkhas*, which may reach up to 1 m on the leeward shore of the playas. In the lateral margins of the lakes, there are trains of *nebkhas*

locally forming ribbons several tens of meters long. These ribbons parallel to the prevalent wind direction are locally remoulded into yardangs.

#### 4. Discussion and evolutionary model

The generation of yardangs results from complex interactions between internal factors (lithology and structure) and external factors (one-directional winds, flow systems surrounding the yardangs and supply of abrading particles) (Greeley and Iversen, 1985). There is also a suite of non-aeolian processes such as gully-ing, salt weathering, cracking, slumping, etc., which contribute to their evolution. The yardangs in the southern sector of the Tibesti desert constitute a good example of the influence of the internal factors. There, the yardangs are restricted to sandstone lithologies (Mainguet, 1968, 1972). Additionally, in that region, the dense jointing controls both the orientation of the yardangs and the width of the corridors. In the studied playa–yardang systems, the abrading particles come primarily from the deflation of particles from the bottom of the playas. As was shown by the geomorphological map, the generation of yardangs requires the existence of large playas, greater than 0.03–0.14 km<sup>2</sup>, e.g., the playas situated to the northeast of El Pito (Fig. 5). Hence, the size of the playas and the time and proportion that they remain flooded are limiting factors in the development of these erosional aeolian landforms.

The geomorphological evolution of the playa–yardang systems on the Bujaraloz platform started with the erosion of a Miocene sequence above the platform (around 250 m thick) and the local exhumation of the structural platform. Most of the surface was exposed prior to the formation of the highest preserved terrace of the Ebro River in the area, since this alluvial level is inset below the platform. During the Pliocene, the Ebro River started to flow into the Mediterranean Sea. Once the soluble sediments of the platform were exhumed, infiltration and downward percolation of meteoric water, to a shallow saturated zone, generated closed depressions (solution dolines) by dissolution processes. Some of the growing dolines have coalesced to form elongated uvalas.

The solution dolines become progressively deeper by epiphreatic dissolution until they reach the water

table, which causes the periodic flooding of the depressions (Sánchez Navarro et al., 1989; Sánchez et al., 1998). The exposure of the saturated zone at the land surface leads to significant evaporation creating a hydraulic gradient towards the saline lake and groundwater flow cells. This situation causes a reversal in the flow of the depressions with rising groundwater towards the playas, preventing the infiltration of meteoric water. The ascending groundwater flowing through the low permeability bedrock supplies solutes to the flat and shallow lakes which precipitate by evaporation (Bowler, 1976; Sánchez Navarro et al., 1989; Sánchez et al., 1998).

The closed depressions constitute local base levels for runoff. This topographic relief favours the development of gullies with internal drainage. A large proportion of the incisions is controlled by WNW–ESE trending fractures (Arlegui and Simón, 2001). The enlargement of the bottom of the playas is produced by several processes including dissolution, salt weathering, gullying, and lateral undercutting at the foot of the depression margins during flooding periods. The undercutting of the basin edges promotes falls and different types of mass wasting processes.

During dry periods the wind mobilises particles from the bed of the playas towards the leeward sectors of the lake basins, sculpturing the yardangs. The gullies in these margins of the depression are widened and deepened by aeolian erosion, giving rise to U-shaped and flat-bottomed valleys or corridors (Laity, 1994). The compression of the flow lines in the corridors causes abrasion on the bottom and slopes (Blackwelder, 1934), whereas the yardangs are located in zones with lower pressure. According to Whitney (1985) and Laity (1994), the corridors are the zones with greatest geomorphic activity in relation to yardang genesis. The progressive widening of the corridors tends to break up the yardangs into smaller landforms, such as mesas, cones, pyramids, etc. (Halimov and Fezer, 1989). The bowl-shaped dolines recognised in the corridors of the study area may have been generated by subsidence caused by subsurface dissolution and/or aeolian deflation.

The yardangs are more frequently developed on plateaus dissected by the drainage net with unidirectional winds (Halimov and Fezer, 1989; Laity, 1994). The gullies parallel to the wind direction are widened

(Breed et al., 1997), whereas wind erosion tends to obliterate the gullies of the windward slopes (Ward and Greeley, 1984).

Nowadays, the origin of the yardangs is quite well understood as a result of experiments carried out in the field and with wind tunnels (Whitney, 1978, 1983; Ward and Greeley, 1984). These studies emphasise the relevance of abrasion and deflation as is also supported by McCauley et al. (1977). The abrupt windward side is experimentally generated by erosion on corners and windward slopes (Ward and Greeley, 1984), whereas Whitney (1983) maintains that they are produced by backward flows from the leeward side. According to Whitney (1985), this negative flow is responsible for the most important erosion in the yardang. Sandblasting is confined to the windward slope and the primary wind causes undercutting and subsequent rock-falls keeping the high inclination of this slope. The abrasion is limited to the saltation transport height which may reach 3 m (Pye and Tsoar, 1990), and is at a maximum at 2 m (Sharp, 1969).

The flow lines surrounding the yardang separate in the leeward side forming turbulence and return flows. This aerodynamic system produces differential pressures giving rise to secondary currents, which transport particles over the surface in suspension. These particles flow towards vorticity centers and act as erosional tools (Whitney, 1978, 1983, 1985). Vorticity is one of the most frequent and important wind movements responsible for the erosion. It acts on the surface of an object along positive, negative and secondary flow lines (Whitney, 1978).

On the extensive Bujaraloz platform, the yardangs are restricted to the leeward margin of the largest playas: La Playa, El Pueyo and El Pito. This spatial relationship is clearly due to the necessity of having a source of aeolian particles to carve the yardangs and corridors. Yardangs are elaborated on gypsum layers. The surficial outcropping of these layers are strongly weathered, where the resulting material is constituted by grains with a weak adhesion. Consequently, the abrading action of the lenticular gypsum particles in suspension is enhanced.

The terrace levels give evidence of several morpho-sedimentary episodes in the evolution of the lakes. The relatively thick deposits of the lacustrine terraces record periods of vertical aggradation. These sedimentary units were probably formed when the

deposits accumulated in the lake basins could not be deflated due to semi-permanent flooding. Besides, the vegetation developed during wet periods would restrict aeolian erosion.

The entrenchment of the system takes place during dry periods. The bottom of the playa is lowered by subsurface dissolution and deflation. The bedrock beneath the lake is transferred to the surface as a solute, precipitated by evaporation and is removed by the wind. Large volumes of sediments can be evacuated from the playas by aeolian deflation through a considerable time span. During the entrenchment episode subsequent to the formation of the most extensive terrace ( $T_2$ ), the large lake that originally linked La Playa and El Pueyo was segmented into two playas. El Pito has also undergone a partial segmentation during this stage (Fig. 5).

There is no doubt that the phases of greater aeolian erosion correspond to the dry periods when the yardangs are modelled and the corridors are deepened and widened. Numerous researchers indicate that the generation of yardangs requires extremely arid climates, minimal soil and vegetation cover, prevalent one-directional winds and a scarce presence of sand (McCauley et al., 1977; Whitney, 1983, 1985; Ward and Greeley, 1984; Halimov and Fezer, 1989; Laity, 1994; Breed et al., 1997; Goudie et al., 1999). McCauley et al. (1977) consider that the yardangs may not persist if the climate changes to more humid conditions. The existence of yardangs in the studied semiarid area could be due to the presence of dry playas, which constitute a good source for particles for the strong local winds. However, at the present time, the rock yardangs are covered by shrub vegetation inhibiting or preventing aeolian erosion. Probably, these landforms originated during dry periods with scarce or non-existent vegetation. The palaeolimnological studies carried out by Schütt and Baumhauer (1996) in the sediments of El Pito playa indicate a change from humid conditions in the lower Holocene to the current semiarid climate within a humid phase within the arid period.

## 5. Age of yardangs

Some authors have estimated erosion rates on yardangs. In Rogers Lake (Mojave Desert), Ward and

Greeley (1984), by means of photographs taken in the field at different dates, estimate that the yardang fronts are eroded by abrasion at rates of 2 cm/year, whereas in the flanks, the erosion by abrasion and deflation reaches 0.5 cm/year. Halimov and Fezer (1989), in Qinghai province, China, based on the content of pottery remains in silt deposits, estimated that small yardangs may form in 1500–2000 years. Clarke et al. (1996) calculated with IRSLS (infra-red stimulated luminescence) on aeolian sands in the Mojave Desert that 1-m high yardangs formed in <250 years. Goudie et al. (1999) calculated in the southwest of Egypt a rate of regional deflation of 1.5 km/ka, assuming a constant vertical downcutting. In the study area, some rubbish dump accumulations have been carved into yardangs. The generation of these landforms may have lasted less than 100 years.

Yardang formation chronology shows important variations in its generation rates. Although yardangs normally developed in extreme arid climates, yardang fields have also been recognised in arid and semiarid climates. In semi-arid areas, the presence of yardangs may be an indication of past climatic change.

## Acknowledgements

The authors would like to thank Prof. Nicholas Lancaster for his helpful and detailed comments and reviews, which have considerably improved this manuscript.

## References

- Arlégui, L., Simón, J.L., 2001. Geometry and distribution of regional joint sets in a non-homogeneous stress field: case study in the Ebro basin (Spain). *J. Struct. Geol.* 23, 293–313.
- Arlégui, L.E., Soriano, M.A., 1996. Lineamientos y su influencia en los modelados del centro de la Cuenca del Ebro. In: Grandal, A., Pagés, J. (Eds.), *IV Reunión Nacional de Geomorfología. Cuadernos do Laboratorio Xeolóxico de Laxe, O Castro (Coruña)*, pp. 11–21.
- Arlégui, L.E., Soriano, M.A., 1998. Characterizing lineaments from satellite images and field studies in the central Ebro basin. *Int. J. Remote Sens.* 19, 3169–3185.
- Ascano, A., Cuadrat, J.M., 1981. El clima. In: Higuera, A. (Ed.), *Geografía de Aragón. Guara, Zaragoza*, pp. 93–140.
- Blackwelder, E., 1934. Yardangs. *Geol. Soc. Am. Bull.* 45, 159–166.
- Bowler, J.M., 1976. Aridity in Australia: age, origins and expression in aeolian landforms and sediments. *Earth Sci. Rev.* 12, 279–310.
- Breed, C.S., McCauley, J.E., Whitney, M.I., Tehakarian, V.P., Laity,

- J.E., 1997. Wind erosion in drylands. In: Thomas, D.S.G. (Ed.), *Arid Zone Geomorphology: Process, Form and Change in Drylands*. Wiley, Chichester, pp. 437–464.
- Clarke, M.L., Wintle, A.G., Lancaster, N., 1996. Infra-red stimulated luminescence dating of sands from the Cronese Basins, Mojave Desert. *Geomorphology* 17, 199–205.
- Cooke, R., Warren, A., Goudie, A., 1993. *Desert Geomorphology*. UCL Press, London, 526 pp.
- Eugster, H.P., Hardie, L.A., 1978. Saline lakes. In: Lerman, A. (Ed.), *Lakes: Chemistry, Geology, Physics*. Springer-Verlag, New York, pp. 237–293.
- García Vera, M.A., 1996. Hidrogeología de Zonas Endorreicas en Climas Semiáridos. Aplicación a Los Monegros. Publicaciones del Consejo de Protección de la Naturaleza de Aragón, Zaragoza, vol. 3, 297 pp.
- Goudie, A.S., 1999. Wind erosional landforms: yardangs and pans. In: Goudie, A.S., Livingstone, I., Stokes, S. (Eds.), *Aeolian Environments, Sediments and Landforms*. Wiley, Chichester, pp. 167–180.
- Goudie, A., Stokes, S., Cook, J., Samieh, S., El-Rashidi, O.A., 1999. Yardang landforms from Kharga Oasis, south-western Egypt. *Z. Geomorphol., Suppl.-Bd.* 116, 97–112.
- Greeley, R., Iversen, J.D., 1985. *Wind as a Geological Process on Earth, Mars, Venus and Titan*. Cambridge Univ. Press, Cambridge, 333 pp.
- Gutiérrez, F., Arauzo, T., Desir, G., 1994. Deslizamientos en el escarpe en yesos de Alfajarín. *Cuat. Geomorfol.* 8, 57–69.
- Halimov, M., Fezer, F., 1989. Eight yardang types in Central Asia. *Z. Geomorphol.* 33, 205–217.
- Hedin, S., 1903. *Central Asia and Tibet*. Charles Scribner and Sons, New York, 2 vols., 608 pp.
- Ibáñez, M.J., 1975. El endorreísmo del sector central de la depresión del Ebro. *Cuad. Invest.* 1, 35–48, Logroño.
- Laity, J.E., 1994. Landforms of aeolian erosion. In: Abrahams, A.D., Parsons, A.J. (Eds.), *Geomorphology of Desert Environments*. Chapman & Hall, London, pp. 506–537.
- Laity, J.E., 1995. Wind abrasion and ventifact formation in California. In: Tchakerian, V.P. (Ed.), *Desert Aeolian Processes*. Chapman & Hall, London, pp. 295–321.
- Liso, M., Ascaso, A., 1969. Introducción al estudio de la evapotranspiración y clasificación climática de la Cuenca del Ebro. *An. Estac. Exp. Aula Dei, C.S.I.C.* 10 Zaragoza, 505 pp.
- Livingstone, I., Warren, A., 1996. *Aeolian Geomorphology: An Introduction*. Longman, Harlow, Essex, 211 pp.
- Mainguet, M., 1968. Le Borkou, aspects d'un modelé éolien. *An. Géogr.* 77, 296–322.
- Mainguet, M., 1972. *Le Modelé des Grès. Problèmes généraux*. Institute Géographique Nationale, Paris, 657 pp.
- Maldonado, C., Gutiérrez-Santolalla, F., Gutiérrez-Elorza, M., Desir, G., 2000. Distribución espacial, morfometría y actividad de la subsidencia por disolución de evaporitas en un campo de dolinas de colapso (valle del Ebro, Zaragoza). *Cuat. Geomorfol.* 14, 9–24.
- McCauley, J.F., 1973. Mariner 9 evidence for wind erosion in the equatorial and mid-latitude regions of Mars. *J. Geophys. Res.* 78, 4123–4137.
- McCauley, J.F., Grolier, M.J., Breed, C.S., 1977. Yardangs. In: Doehring, D.O. (Ed.), *Geomorphology in Arid Regions*. Allen and Unwin, London, pp. 233–269.
- McCauley, J.F., Breed, C.S., El-Baz, F., Whitney, M.I., Grolier, M.J., Ward, A.W., 1979. Pitted and fluted rocks in the Western Desert of Egypt—Viking comparisons. *J. Geophys. Res.* 84, 8222–8232.
- Pueyo, J.J., 1978. La precipitación evaporítica actual en las lagunas saladas del área: Bujaraloz, Sástago, Caspe, Alcañiz y Calanda (provincias de Zaragoza y Teruel). *Rev. Inst. Invest. Geol.* 33, 5–56, Barcelona.
- Pueyo, J.J., 1980. Procesos diagenéticos observados en las lagunas tipo playa de la zona de Bujaraloz-Sástago (provincias de Zaragoza y Teruel). *Rev. Inst. Invest. Geol.* 34, 195–207, Barcelona.
- Puircerús, J.A., Valero, A., Navarro, J., Terrén, R., Zubiaur, R., Martín, F., Iniesta, G., 1994. *Atlas Eólico de Aragón*. Gobierno de Aragón, Zaragoza, 127 pp.
- Pye, K., Tsoar, H., 1990. *Aeolian Sand and Sand Deposits*. Unwin Hyman, London, 396 pp.
- Quirantes, J., 1965. Nota sobre las lagunas de Bujaraloz-Sástago. *Geographica* 12, 30–34.
- Quirantes, J., 1978. Estudio Sedimentológico y Estratigráfico del Terciario Continental de los Monegros. Institución Fernando el Católico, C.S.I.C., Zaragoza, 200 pp.
- Ramírez, J.I., 1997. Mapa Geológico de España a Escala 1:50000, Gelsa (n° 413). Instituto Tecnológico Geominero de España, Madrid.
- Salvany, J.M., García Vera, M.A., Samper, J., 1994a. Influencia del sustrato terciario en el emplazamiento del complejo lagunar de Bujaraloz (Monegros, Cuenca del Ebro). *Actas II Congr. Esp. Terciario*. Jaca, 271–274.
- Salvany, J.M., Muñoz, A., Pérez, A., 1994b. Nonmarine evaporitic sedimentation and associated diagenetic processes of the south-western margin of the Ebro Basin (Lower Miocene), Spain. *J. Sediment. Res. A* 64, 190–203.
- Salvany, J.M., García Vera, M.A., Samper, J., 1996. Geología e hidrogeología de la zona endorreica de Bujaraloz-Sástago (Los Monegros, provincia de Zaragoza y Huesca). *Acta Geol. Hisp.* 30, 31–50.
- Sánchez Navarro, J.A., Martínez Gil, F.J., de Miguel Cabeza, J.L., San Román, J., 1989. Hidrogeoquímica de la zona endorreica de las lagunas de Monegros, provincias de Zaragoza y Huesca. *Bol. Geol. Min.* 100, 876–885.
- Sánchez, J.A., Pérez, A., Coloma, P., Martínez Gil, J., 1998. Combined effects of groundwater and aeolian processes in the formation of the northernmost closed saline depressions of Europe: north-east Spain. *Hydrol. Processes* 12, 813–820.
- Sharp, R.P., 1969. Wind-driven sand in Coachella Valley, California. *Geol. Soc. Am. Bull.* 75, 785–804.
- Solá, J., Costa, J.M., 1997. Mapa Geológico de España a Escala 1:50000, Bujaraloz (n° 414). Instituto Tecnológico Geominero de España, Madrid.
- Schütt, B., Baumhauer, R., 1996. Playa sedimente aus dem Zentralen Ebrobecken/Spanien als Indikatoren für holozäne klimaschwankungen-ein vorläufige Bericht. *Petermans Geogr. Mitt.* 140, 33–42.
- Ward, A.W., 1979. Yardangs on Mars: evidence of recent wind erosion. *J. Geophys. Res.* 84, 8147–8166.

- Ward, A.W., Greeley, R., 1984. Evolution of the yardangs at Rogers Lake, California. *Geol. Soc. Am. Bull.* 95, 829–837.
- Whitney, M.I., 1978. The role of vorticity in developing lineation by wind erosion. *Geol. Soc. Am. Bull.* 89, 1–18.
- Whitney, M.I., 1983. Eolian features shaped by aerodynamic and vorticity processes. In: Brookfield, M.E., Ahlbrandt, T.S. (Eds.), *Eolian Sediments and Processes*. Elsevier, Amsterdam, pp. 223–245.
- Whitney, M.I., 1985. Yardangs. *J. Geol. Educ.* 33, 93–96.